journal

Reprinted from the Journal of the American Ceramic Society, Vol. 79, No. 3, March 1996

J. Am. Ceram. Soc., 79 [3] 634–40 (1996)

Crack Suppression in Strongly Bonded Homogeneous/Heterogeneous Laminates: A Study on Glass/Glass-Ceramic Bilayers

Sataporn Wuttiphan† and Brian R. Lawn*

Materials Science and Engineering Laboratory, National Institute of Standards and Technology, Gaithersburg, Maryland 20899

Nitin P. Padture*

Department of Metallurgy and Institute of Materials Science, University of Connecticut, Storrs, Connecticut 06269

A study is made of a glass/glass-ceramic bilayer as a model homogeneous/heterogeneous laminate. The underlying objective is microstructural design of ceramic layer systems with optimum mechanical properties, alternating hard layers, for wear resistance, with tough layers, for fracture resistance. Mica flakes in the glass-ceramic layer inhibit the propagation of well-developed intrusive cracks, by bridging; these same flakes render the structure susceptible to distributed damage, by providing discrete weakness at the microstructural level. A major distinguishing feature of the bilayer design is the incorporation of a strong interface, so that cracks are inhibited by the underlayer rather than deflected between the layers. Vickers and Hertzian indentation tests on specimen cross sections demonstrate the capacity of the glass-ceramic layer to arrest radial and cone cracks penetrating from the adjacent glass layer. Additional Hertzian tests on the outer surfaces of glass layers in a coating/substrate configuration show diffuse damage accumulation in the glass-ceramic substrate layers. This diffuse damage absorbs energy and shields cone cracks in the glass from the applied loading. Implications concerening the design of damage-tolerant laminate structures are discussed.

I. Introduction

BILAYER and multilayer ceramic laminate structures have been proposed as a means of counteracting brittleness in tensile loading by deflection of cross-member cracks along an orthogonal interlayer path.[1–8] Delamination cracks of this kind are readily amenable to fracture mechanics analysis, by regarding each member of the laminate as a continuum slab separated from its neighbors by weak interfaces. However, delamination does not always guarantee immunity to premature failure, especially when the loading has some bending or longitudinal compression component. Consequently, conventional laminates are subject to severe restrictions on their usage in structural applications.

Here we adopt an alternative laminate design approach, based on crack suppression rather than crack deflection. The idea is to interleave hard homogeneous layers, for good wear resistance, with tough heterogeneous microstructures, for good fracture resistance. The interfaces between adjacent layers are strongly bonded, to discourage delamination. Cracks in the homogeneous layers then penetrate the interfaces, to be absorbed or arrested in the adjacent heterogeneous layers. This philosophy has been foreshadowed to a certain extent in crack propagation studies on ceramic/metal laminates[9] and on some tailored ceramic/ceramic laminates.[10–14] It has been demonstrated compellingly in Hertzian contact tests on an alumina/alumina:calcium–hexaluminate trilayer composite system, in which cone crack propagation in the outer homogeneous (alumina) layer is suppressed by quasi-plastic damage in the inner heterogeneous (alumina:calcium–hexaluminate) layer, to the extent that the cone cracks never intersect the interface.[15] This leaves open the question as to the crack response once intersection ever could be made to occur: would the crack be simply impeded by the tough underlayer, dispersed into a microcrack cloud, or deflected regardless along the interface?

In the present paper we seek to gain answers to such questions by constructing a model homogeneous/heterogeneous laminate system, in the form of a glass/glass-ceramic bilayer. For the heterogeneous component, we use a mica-containing glass-ceramic with weak interphase boundaries, with capacity for distributed damage accumulation[16] yet with respectable long-crack toughness. For the glass, we use soda–lime for low thermal expansion mismatch with the glass-ceramic, to avoid complications from macroscopic residual stresses. Microstructurally, these two materials lie at opposite extremes of the homogeneous–heterogeneous spectrum: in Hertzian contacts on bulk specimens, the glass produces cone fractures typical of classical brittle solids, whereas the glass-ceramic produces subsurface quasi-plastic damage more typical of plastic solids.[16,17] The two materials are hot-pressed together to form a well-defined, strongly bonded interface. Hertzian and Vickers indentations are used to introduce controlled cracks in the glass layer close to the interface. In some configurations these cracks can be made to penetrate the interface, and in those cases continued propagation is inhibited by bridging from the mica flakes in the glass-ceramic. In other configurations the cracks remain wholly contained in the glass layer, shielded by a distributed damage zone in the glass-ceramic layer. Implications concerning the design of microstructures for optimum interlayer synergism in the fracture suppression are considered.

II. Experimental Procedure

Model composite systems of soda–lime glass and a glass-ceramic with composition ≈55% fluorophlogopite mica and ≈45% borosilicate glass (Macor, Corning Inc., Corning, NY)[18,19,‡] were prepared by fusing bars into bilayers. In the

K. Jakus—contributing editor

Manuscript No. 192562. Received June 2, 1995; approved October 16, 1995.
Supported in part by the U.S. Air Force Office of Scientific Research; additional support for S. Wuttiphan was provided by a Royal Thai Scholarship.
*Member, American Ceramic Society.
†Graduate Student in the Department of Materials and Nuclear Engineering, University of Maryland, College Park, Maryland 20742.

‡Composition (weight percent): SiO_2 (46%), MgO (17%), Al_2O_3 (16%), K_2O (10%), B_2O_3 (7%), F (4%).

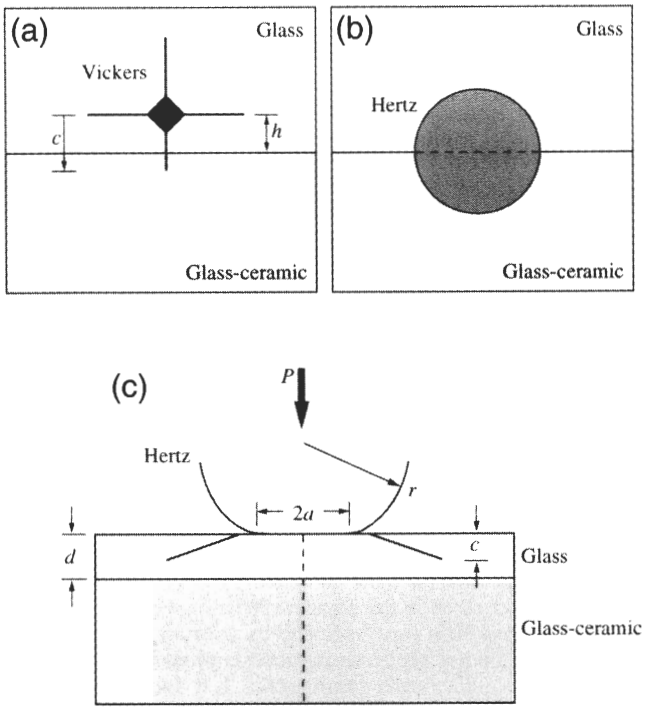

Fig. 1. Schematic depicting indentations in glass/glass-ceramic bilayer system: (a) Vickers indentation in side surface of glass layer, propagating radial crack across bilayer interface; (b) Hertz indent made symmetrically across similar glass/glass-ceramic interface; (c) Hertz indentation made in top surface glass layer, so that cone crack extends downward toward glass-ceramic sublayer.

heterogeneous glass-ceramic the mica is in platelet form with weak interphase boundaries, with consequent easy fracture at the microstructural level ("machinable" glass-ceramic).[18–20] At the same time, the mica platelets act effectively as bridges on larger cracks,[21] leading to a rising toughness curve and enhancing long-crack toughness.[22] The homogeneous soda–lime glass has the same nominal thermal expansion coefficient as the glass-ceramic to within 1% ($9.4 \times 10^{-6}\ °C^{-1}$), thereby avoiding significant residual mismatch stresses in the final composite.

To form the glass/glass-ceramic bilayers, the bulk materials were first cut into slabs 25 mm × 25 mm × 3 mm, and polished to 1 μm finish on one face. Glass and glass-ceramic slabs were placed into mutual contact at their polished faces, and then cosintered at 700°C and 30 MPa for 15 min in argon gas. The ensuing interface between the two layers was well-defined, with no visible voids.

Specimens were prepared from the as-sintered bilayers for indentation testing. In one configuration, a test surface was polished normal to the layer interface (section configuration, Figs. 1(a) and (b)). In another, the glass layer was cut parallel to the layer interface, surface-ground, and polished to a thickness of 300 μm (coating/substrate configuration, Fig. 1(c)). A variant of this latter configuration was prepared by bonding together two half-specimens with adhesive to form a *bonded* interface normal to the *layer* interface (dashed line in Fig. 1(c)) for subsequent viewing of subsurface damage.[16,23]

Indentation tests were made on the specimen surfaces as follows:

(i) Vickers Tests on Section Specimens, Fig. 1(a): Vickers indentations were made in the glass layer, over a load range $P = 20$–100 N, in air. The pyramidal indenter was oriented so that the radial cracks were aligned parallel and perpendicular to the interface. Three series of indentations were made along prescribed lines at distances $h = 100$, 200, and 300 μm from the interface, so that the lower radial crack might be induced to penetrate the interface into the glass-ceramic. After the specimens were left in laboratory atmosphere for 1 day, the indented surfaces were gold coated for viewing in Nomarski interference illumination in an optical microscope. High-magnification measurements were made of the radial crack sizes c for each of the radial arms at each load P and distance h. Some dummy tests were also run on surfaces of bulk glass specimens, to provide a comparison baseline for data analysis.

(ii) Hertzian Tests on Section Specimens, Fig. 1(b): Hertzian indentations were made with a tungsten carbide sphere of radius 3.18 mm, again in air. In this case the contacts were made symmetrically across the glass/glass-ceramic interface trace. Two series of tests were made: first, single-cycle at loads $P = 500$, 700, and 1200 N; second, multiple-cycle, $n = 10$, 10^3, and 10^5 cycles, at constant load 500 N. Again, the indented surfaces were gold coated for viewing in Nomarski interference illumination.

(iii) Hertzian Tests on Coating/Substrate Specimens, Fig. 1(c): Hertzian indentations were made under loading conditions similar to those in (ii) above but on the top glass surface instead of the section surface. To observe subsurface damage, indentations were made along traces of bonded interfaces, i.e., symmetrically across the dashed line in Fig. 1(c). After the indented specimen halves were separated in solvent,[23] a gold coat was once more applied to the side surfaces for viewing in Nomarski contrast.

III. Results

(1) Vickers Indentations: Section Configuration

Consider first the Vickers indentations in the section configuration of Fig. 1(a). Micrographs of the ensuing radial crack system are shown in Fig. 2 for loads $P = 20$, 60, and 100 N. A well-defined radial crack system is evident in each case. Invariably, the cracks continued to extend after indentation, indicating slow crack growth, although the bulk of this persistent extension was realized after the 1-day postindentation delay prior to crack measurement.[24,25] At the lowest load shown (Fig. 2(a)), all four radial cracks remain fully contained within the glass layer. At the higher loads (Figs. 2(b) and (c)), the lower radial crack penetrates the interlayer interface continuously (i.e., without reinitiation) into the glass-ceramic layer. Those cracks that remain wholly contained in the glass are indistinguishable in lengths from corresponding cracks in dummy tests on bulk glass, within ≈5% standard deviation (see Fig. 3), and are relatively straight, confirming the absence of any significant residual stresses from thermal expansion anisotropy.

By contrast, the radial cracks penetrating into the glass-ceramic are substantially shorter, indicating an inhibiting effect on propagation from bridging. Such bridging was apparent in higher-magnification examinations of the crack walls.[21] No suggestion of interlayer delamination was evident in any of the Vickers indentation tests, confirming the presumption of a strongly bonded interlayer interface. Nor was there any suggestion that the penetrating radial cracks ever disperse into a microcrack cloud or branch zone in the tip region, even though the Macor glass-ceramic has the prime qualities of exceptionally weak and highly stressed mica/glass internal interfaces for such dispersion.[16,18,19]

A quantitative evaluation of the radial crack length data may be made in terms of the residual stress-intensity factor

$$K_r(c) = \chi P/c^{3/2} \tag{1}$$

where χ is an indentation coefficient representing the intensity of the residual elastic-plastic stress field around the Vickers indentation.[24,26] Since the Vickers impressions are contained wholly in the glass layer, the appropriate value of χ is that for bulk glass. Under inert conditions, crack lengths are determined by the equilibrium condition $K_r(c) = T$, where T refers to the toughness of the material containing the crack tip. In the present tests in air, the persistent postindentation crack extension causes $K_r(c)$ to equilibrate at some level lower than T. Moreover, the

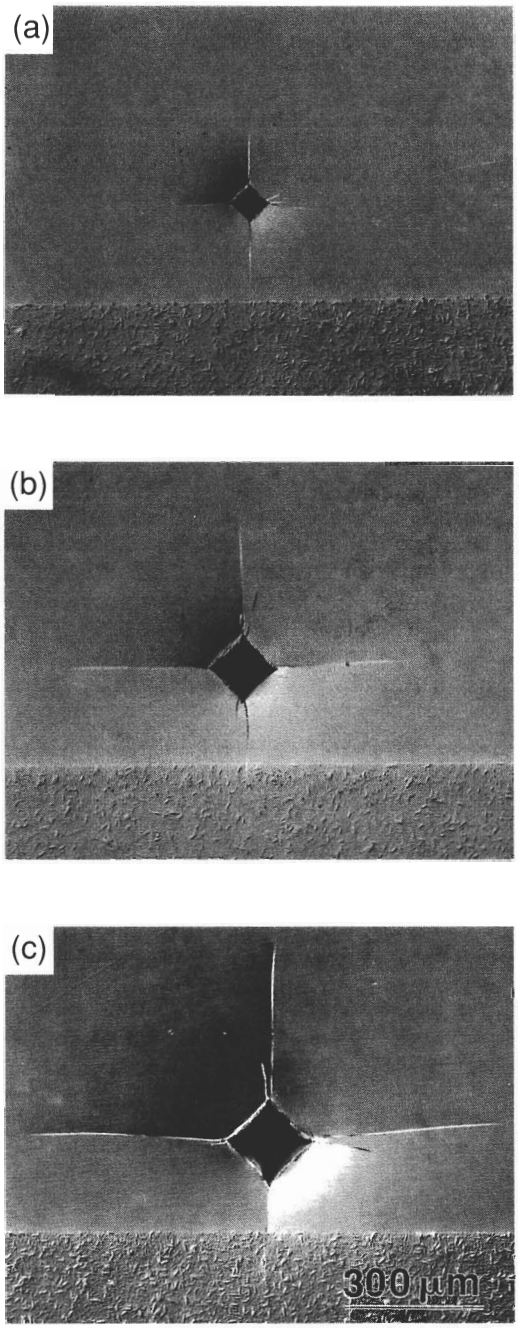

Fig. 2. Micrographs of Vickers radial crack systems in glass side surface at distance h = 200 μm from glass/glass-ceramic bilayer interface, tests in air. Indentations at loads (a) P = 20 N, (b) 60 N, and (c) 100 N. Note how lower radial crack approaches and penetrates interface, arresting in the glass-ceramic.

residual contact field is subject to diminution from postindentation relaxation.[25] This relaxation is allowed for in some measure in indentation–strength tests, in which strengths are measured on bars containing aged Vickers cracks. Accordingly, we use earlier indentation–strength data[27] to evaluate χ = 0.028 for soda–lime glass (Appendix). With further regard to T, we note that only that portion of the radial crack arm contained in the glass-ceramic is subject to bridging by the mica grains, so it is expedient to refer all toughness data to an origin at the interface, i.e., relative to a coordinate c–h (Fig. 1).

Accordingly, a plot of the $K_r(c-h)$ data for the bilayer glass/glass-ceramic system is shown in Fig. 3. The horizontal solid line at left represents the mean value of K_r from the dummy tests on bulk glass specimens. Included as the dashed curves are independently determined toughness levels for equilibrium

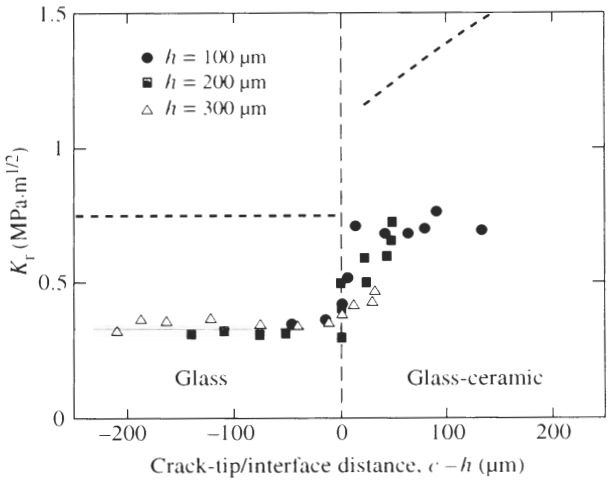

Fig. 3. Plot of residual stress-intensity factor for Vickers indentations in glass and radial cracks in glass-ceramic, tests in air. Data points are from crack size measurements at different loads P and distances h from interface. Broken curves are independently determined toughness values for glass[28] and toughness curve for glass-ceramic (Appendix) under inert testing conditions. Horizontal solid line at left is K_r determination from surfaces of bulk glass specimens.

crack growth; at left, for glass, T_0 = 0.75 MPa·m$^{1/2}$;[28] at right, for Macor glass-ceramic, $T(c)$ objectively deconvoluted from earlier Vickers indentation–strength data on this material[22] (Appendix). Observe that the data lie below the dashed curves, consistent with a reduction in K_r from moisture-assisted crack growth. It is apparent that, notwithstanding the influence of moisture, the penetrating crack is significantly impeded by the tough sublayer. Thus, whereas the toughness remains invariant for crack propagation in the glass, it rises in a toughness curve as the crack crosses the interface and suffers cumulative inhibition by bridging stresses.

(2) Hertzian Indentations: Section Configuration

Micrographs of Hertzian cracks in the section configuration of Fig. 1(b) are shown in Fig. 4 for single-cycle contact at increasing load and in Fig. 5 for an increasing number of cycles at constant contact load. In conventional Hertzian tests on bulk glass, cone cracks initiate at some point outside the contact and run down and around in the axisymmetric stress field to close the circular ring on the opposite side.[29] In the bilayer system in Figs. 4 and 5, initiation again occurs in the glass layer, but the ensuing axisymmetric propagation is interrupted by the glass-ceramic layer. As with the Vickers indentations, the cracks penetrate the interlayer interface as continuous entities. On increasing the contact load (Fig. 4) or number of cycles (Fig. 5) multiple concentric cracks are initiated,[30] from a combination of increased stress intensity and moisture-assisted crack growth. In the case of multiple loading (Fig. 5(c)) "fretting" damage from reversed slip at the contact surface[31] contributes to the increased damage severity. However, the degree of crack penetration into the adjacent layer does not appear to show any corresponding increase, attesting further to the crack-arrest capacity of the glass-ceramic. Again, there is no evidence of any delamination at the strong glass/glass-ceramic interface.

Simultaneous with the cone crack arrest is the development in the glass-ceramic of a quasi-plastic contact impression, from distributed microfailures of mica/glass interfaces.[16,32] Hence the heterogeneity in the microstructure effects a kind of transition from well-defined fracture to diffuse damage.[17] Again, this diffuse zone is associated with the contact field, and not with a crack-tip frontal cloud.

(3) Hertzian Indentations: Coating/Substrate Configuration

Damage patterns from Hertzian contacts in the coating/substrate configuration of Fig. 1(c) are shown in Fig. 6, for

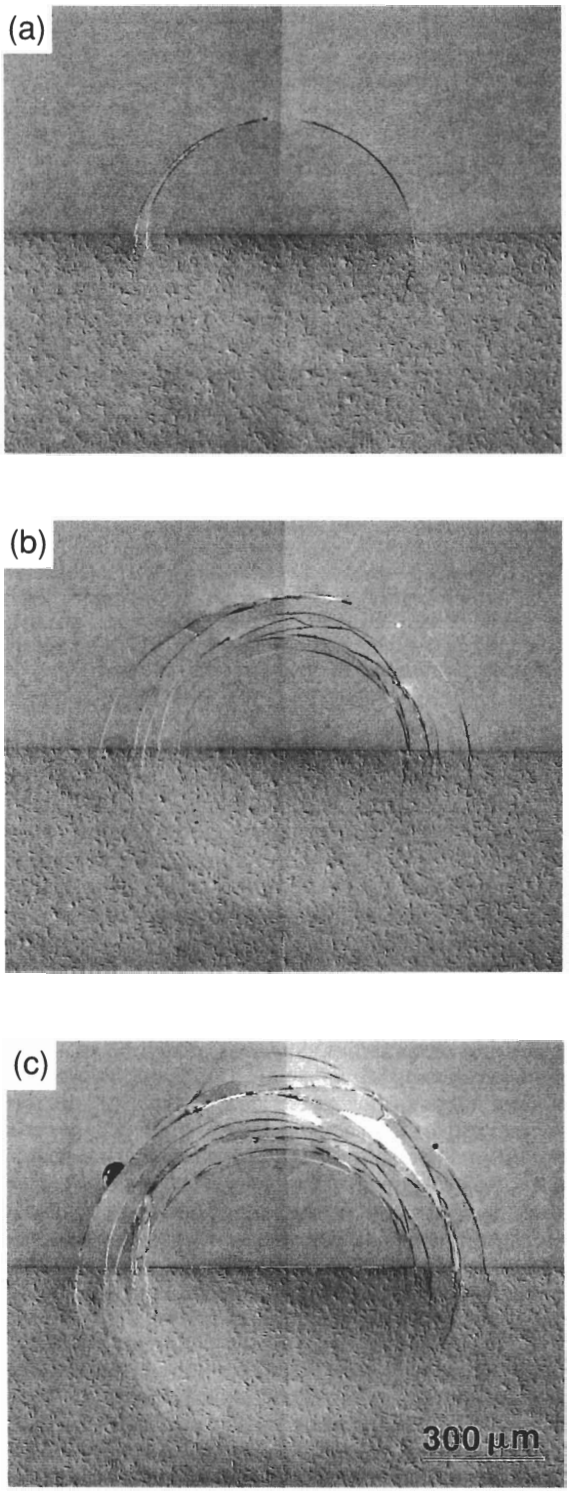

Fig. 4. Hertzian indentations in glass side surface of glass/glass-ceramic bilayer made symmetrically across interface trace, sphere radius r = 3.18 mm. Indentations for single-cycle contact at loads (a) P = 500 N, (b) 700 N, and (c) 1200 N, in air.

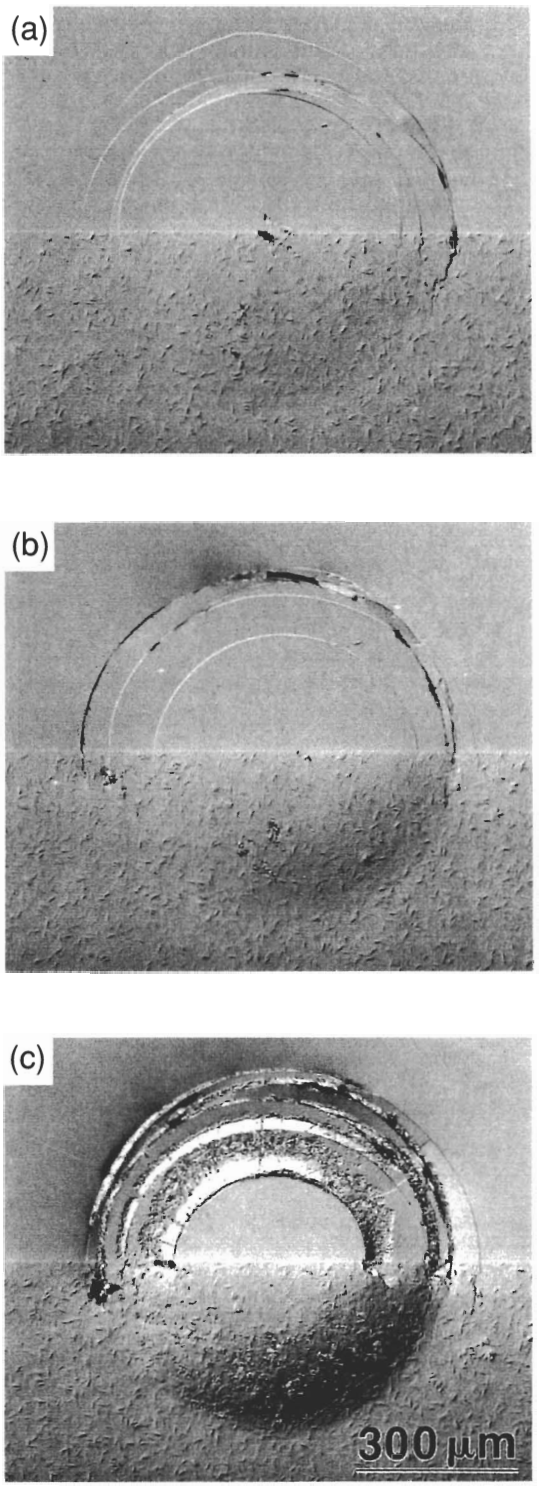

Fig. 5. As in Fig. 4, but at constant load 500 N (cf. Fig. 4(a)) for multiple cyles (a) n = 10, (b) 10^3, and (c) 10^5, in air.

indentations at loads P = 200, 350, and 700 N on bonded-interface specimens. Again, no interfacial delamination is evident. Cone fractures in the top glass layer, and diffuse quasi-plastic damage in the glass-ceramic underlayer, are evident in the micrographs. Once formed, the cone fractures are highly stable. At the lowest load (Fig. 6(a)) a single cone approaches the underlayer. At the intermediate load (Fig. 6(b)) additional cones develop, but do not appear to extend much further in depth. At the highest load (Fig. 6(c)) several cones have formed, but again penetration appears to be restricted. Hence the primary effect of increased loading is to increase the density rather than the depth of the cone cracks. At the same time as the cone fractures proliferate, a second set of stable cracks appears in the glass (Fig. 6(b)) and extends vertically upward toward the top surface from the interface (Fig. 6(c)). Examination of the subsurface contact areas through the top surface of the transparent glass coating indicates that these cracks extend upward as shallow planar segments. At very high loads, above ≈1000 N, one or other of these cracks finally traverses the top layer, and the coating fails.

As indicated, an important feature of the total mechanical response is the quasi-plastic damage zone that forms in the glass-ceramic underlayer. This zone forms immediately adjacent to the interface, and expands with increasing load. At the lowest load (Fig. 6(a)) the zone is barely visible; by the time it reaches the highest load (Fig. 6(c)) it has expanded markedly, to a depth in the underlayer comparable with the coating thickness itself. The deformation within this zone inevitably absorbs mechanical energy, and thereby "shields" the cone crack from the external loading system.[15] This accounts for the constraining effect on cone crack penetration. Again, the role of the damage zone in the initiation and propagation of the secondary cracks remains to be determined.

IV. Discussion

We have proposed a novel approach to the design of crack-inhibiting laminate structures, interleaving hard, homogeneous outer layers with tough, heterogeneous inner layers, using a glass/glass-ceramic layer as a model system for study. Instead of making the interface weak, to deflect cracks, we seek to make the interface strong, to allow penetration of the cracks into the tough underlayer. The tough underlayer then absorbs or disperses the penetrating cracks. Key to the materials design is tailoring of the microstructure for quasi-plasticity in the contact response. As we have seen, the same microstructural elements that are requisite for such "plasticity" are those responsible for the toughness of the material. In the mica-containing glass-ceramic, it is the weak interfaces between the mica platelets and the glass matrix that allow for intrinsic shear deformation in the subsurface Hertzian field[16,17] and at the same time facilitate bridging in well-developed cracks. Thus the notion of delamination is not entirely eliminated: rather, delamination occurs over many microscopically confined, discrete shear "faults" within the deformation zone instead of macroscopically along a continuous interlayer interface.

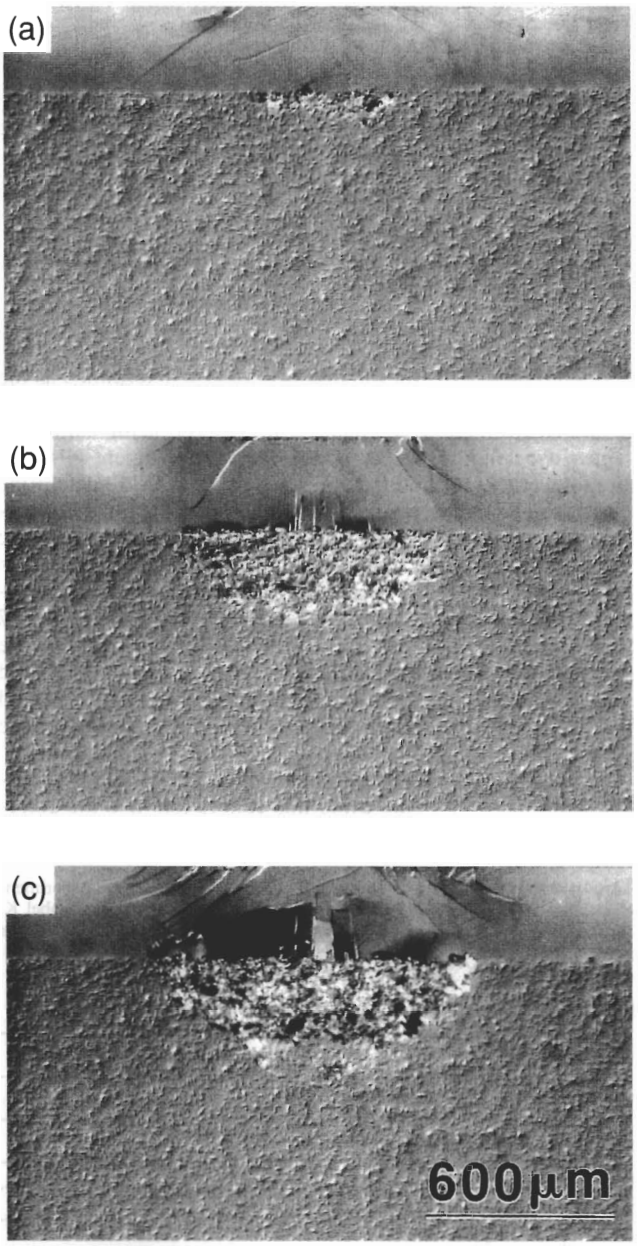

Fig. 6. Hertzian indentations in top glass surface, thickness 300 μm, on glass/glass-ceramic bilayer. Tests at loads (a) $P = 200$ N, (b) 350 N, and (c) 700 N, sphere radius $r = 3.18$ mm. Note expansion of diffuse damage zone in heterogeneous sublayer with increasing load, and corresponding increase in density but not depth of cone cracks in top glass layer.

The Vickers indentation test results summarized in Figs. 2 and 3 are useful for highlighting the role of a tough underlayer in suppressing crack propagation in laminate structures. In the Vickers tests, radial cracks initiate from the indentation corners in the glass and retain their well-developed character as they penetrate the glass/glass-ceramic interface. Within the sublayer the cracks are inhibited by bridging, by heterogeneities in the microstructure. Measurements of the radial crack sizes verify the existence of a rising toughness curve in the glass-ceramic. The effect of the sublayer on crack inhibition is not dissimilar to that observed in the work of Marshall and co-workers on alumina/zirconia laminates,[12,13] although in that system the toughening is due to phase transformation in Ce-TZP layers. No microcrack cloud is detected around the crack tip in the observations in Fig. 2, even though the glass-ceramic contains weak mica–glass interfaces that might be considered most conducive to microcracking.

The Hertzian indentation tests serve both to reinforce the Vickers results and to provide insight into alternative modes of deformation in the sublayer when crack penetration is suppressed. In the section configurations of Figs. 4 and 5, we see further indication of the capacity of the tough glass-ceramic layer to inhibit and arrest penetrating cracks. Additionally, we see the capacity of this same layer to absorb energy by creation of a quasi-plastic deformation zone beneath the contact. The latter process is seen to even greater effect in the coating/substrate configuration of Fig. 6, with the expansion of an ever-increasing sublayer damage zone as load increases. It is interesting to note in passing that the critical load for onset of this zone, ≈200 N (Fig. 6(a)), is comparable with that observed previously in the bulk glass-ceramic, ≈250 N (Fig. 4(a), Ref. 16), as might be expected for a coating/substrate system with near-matching elastic modulus.[16] The energy absorption associated with the damage "shields" the cone cracks in the outer layer from the applied indentation load, thereby suppressing crack penetration into the sublayer.[15] At the same time, the density of cone cracks increases with load, and a set of secondary cracks begins to extend stably upward from the glass/glass-ceramic interface toward the specimen surface. At some overload condition, one or both of the downward penetrating cone cracks or upward extending secondary cracks traverses the thickness of the outer layer, and coating failure ultimately occurs.

As indicated in Section III(3), a more detailed study of the constrained cone cracks and secondary cracks remains to be carried out. Any such study must start with a proper analysis of the elastic–plastic contact stress field in the layer structure. Analyses of this kind are not amenable to closed-form solution, so numerical computational techniques are required. Existing finite element calculations for hard coatings on metal substrates indicate the important role of elastic–plastic mismatch, specifically in redistributing the shear stress concentrations immediately below the interface where plasticity occurs.[33] Similar

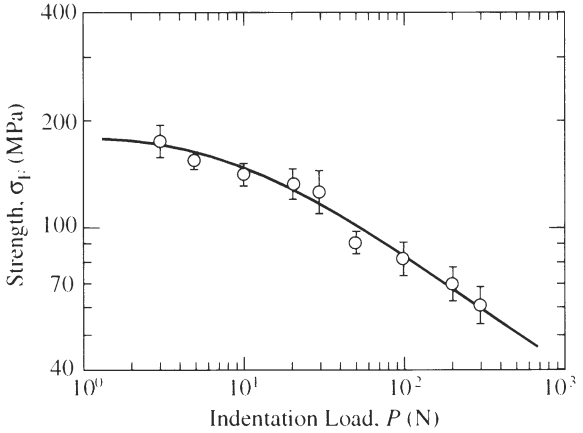

Fig. A1. Inert strength as function of Vickers indentation load for Macor glass-ceramic. Data from Ref. 22.

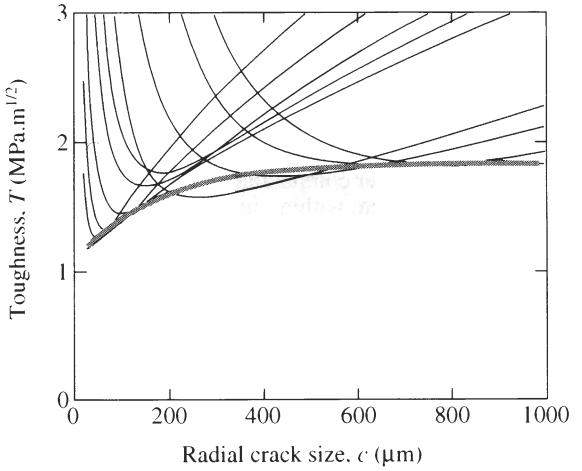

Fig. A2. Deconvolution of toughness curve for Macor glass-ceramic from indentation–strength data in Fig. A1. $T(c)$(thick line) is determined as envelope of $K'_A(c)$ curves (thin lines).

calculations are also needed to determine the redistributions of tensile stresses in the coating where cracking occurs.

It is interesting to examine the indentation conditions under which we may expect the kind of sublayer damage seen in Fig. 6 to occur. Experiments on bulk ceramics subject to such damage indicate that, as a rule of thumb, quasi-plastic damage zones extend to a depth of about one contact diameter.[16,17,23,34,35] Relative to the coating thickness $d = 300$ μm, the contact diameters in Figs. 6(a–c) are $2a = 380$, 460, and 590 μm, respectively. Accordingly, an approximate condition for the contact near field to encompass the sublayer is $2a > d$ (notwithstanding any modifications from elastic–plastic mismatch), a condition most readily achieved for any given contact system by suitably reducing the coating or laminate thickness.

Although we have focused our attention on one model bilayer system with relatively small elastic mismatch (glass/glass-ceramic), and on one specific kind of crack system with unusually high stability (indentation cracks), the implications concerning laminate design through microstructural design would appear to have a certain generality. As indicated, the approach is to interleave hard homogeneous layers with tough heterogeneous layers, with strongly bonded interfaces. The hard component is placed on the outer surface, to provide wear resistance. The tough component forms the underlayer, to provide fracture resistance if crack penetration occurs or, better still, to suppress penetration by energy absorption within a sublayer damage zone. The key to the design of the tough component is the incorporation of elements of microstructural weakness, to enhance formation of bridges across an entrant crack and to promote discrete shear failures within a diffuse quasi-plastic damage zone. Such elements, by distributing the fractures discretely within the subsurface contact volume, are essential ingredients for enhanced damage tolerance[35] and reduced strength degradation.[16] The issue of optimum layer thickness needs to be considered in this light: thus, the brittle outer layer must be thin enough that the plastic sublayer "intercepts" the contact near field, yet not too thin that the cone and secondary fractures cause premature failure.

APPENDIX

Deconvolution of Toughness Curve for Glass-Ceramic from Indentation–Strength Data

Here we deconvolute the toughness curve, $T(c)$, for the Macor glass-ceramic used in the present work, using Vickers indentation–strength data from an earlier study on the same material.[22] The inert strengths σ_M from that earlier study are plotted as a function of indentation load P in Fig. A1.

The deconvolution follows an objective procedure described by Braun *et al.*[36] The effective applied stress-intensity factor $K'_A(c)$ for an equilibrium Vickers indentation produced at load P and subjected to a subsequent flexural stress σ_A may be written as the following function of radial crack size c:

$$K'_A(c) = \psi\sigma_A c^{1/2} + \chi P/c^{3/2} = T(c) \qquad \text{(A-1)}$$

with $T(c)$ the T-curve for the material. The "inert strength" $\sigma_A = \sigma_F$ then identifies with the condition for unlimited instability of the radial crack:[37]

$$dK'_A(c)/dc = dT(c)/dc \qquad \text{(A-2)}$$

Accordingly, $T(c)$ for the glass-ceramic is determined as the envelope of tangency points to the family of $K'_A(c)$ curves generated from the $\sigma_F(P)$ data set in Fig. A1, using calibrated values of ψ and χ. The generic geometrical coefficient $\psi = 0.77$ for radial cracks is obtained directly from Ref. 36. To determine the material-specific residual-field coefficient χ for the glass-ceramic, we refer to soda–lime glass as a baseline material: using the appropriate indentation–strength relation $\sigma_M P^{1/3} = (3T_0/4\psi)(T_0/4\chi)^{1/3}$ for materials with single-valued toughness,[36,38,39] in conjunction with experimental data $\sigma_F P^{1/3} = 137$ MPa·N$^{-1/3}$ (Ref. 27) and $T_0 = 0.75$ MPa·m$^{1/2}$ (Ref. 28), we evalulate $\chi = 0.028$ for glass. Then since $\chi = (E/H)^{1/2}$,[26] and with $E = 70$ GPa and $H = 5.5$ GPa for glass, $E = 63$ GPa and $H = 3.0$ GPa for glass-ceramic, we obtain $\chi = 0.037$ for the glass-ceramic.

Figure A2 shows the family of inverted $K'_A(c)$ curves generated from the $\sigma_F(P)$ data using this calibration, and the corresponding $T(c)$ envelope for the glass-ceramic.

Acknowledgments: S. Wuttiphan gratefully acknowledges experimental assistance from Antonia Pajares and much encouragement from Isabel K. Lloyd. Kenneth Chyung, from Corning Glass, kindly provided the Macor specimens.

References

[1]J. Cook and J. E. Gordon, "A Mechanism for the Control of Crack Propagation in All-Brittle Systems," *Proc. R. Soc. London*, **A282**, 508–20 (1964).

[2]K. Kendall, "Transition Between Cohesive and Interface Failure in a Laminate," *Proc. R. Soc. London*, **A344**, 287–302 (1975).

[3]V. J. Laraia and A. H. Heuer, "Novel Composite Microstructure and Mechanical Behavior of Mollusk Shells," *J. Am. Ceram. Soc.*, **72** [11] 2177–79 (1989).

[4]J. W. Hutchinson, "Mixed-Mode Fracture Mechanics of Interfaces"; pp. 295–306 in *Metal–Ceramic Interfaces*. Edited by M. Rühle, A. G. Evans, M. F. Ashby, and J. P. Hirth. Pergamon Press, New York, 1990.

[5]J. W. Hutchinson and Z. Suo, "Mixed-Mode Cracking in Layered Structures," *Adv. Appl. Mech.*, **29**, 64 (1991).

[6]W. J. Clegg, K. Kendall, N. M. Alford, T. W. Button, and J. D. Birchall, "A Simple Way to Make Tough Ceramics," *Nature (London)*, **347**, 455–57 (1991).

[7]C. A. Folsom, F. W. Zok, and F. F. Lange, "Flexural Properties of Brittle Multilayer Materials: I, Modeling," *J. Am. Ceram. Soc.*, **77** [3] 689–96 (1994).

[8]C. A. Folsom, F. W. Zok, and F. F. Lange, "Flexural Properties of Brittle Multilayer Materials: II. Experiments," *J. Am. Ceram. Soc.*, **77** [8] 2081–87 (1994).

[9]M. C. Shaw, D. B. Marshall, M. S. Dadkhah, and A. G. Evans, "Cracking and Damage Mechanisms in Ceramic/Metal Multilayers," *Acta Metall.*, **41** [11] 3311–22 (1993).

[10]C. J. Russo, M. P. Harmer, H. M. Chan, and G. A. Miller, "Design of a Laminated Ceramic Composite for Improved Strength and Toughness," *J. Am. Ceram. Soc.*, **75** [12] 3396–400 (1992).

[11]M. P. Harmer, H. M. Chan, and G. A. Miller, "Unique Opportunities for Microstructural Engineering with Duplex and Laminar Ceramic Composites," *J. Am. Ceram. Soc.*, **75** [7] 1715–28 (1992).

[12]D. B. Marshall, J. J. Ratto, and F. F. Lange, "Enhanced Fracture Toughness in Layered Microcomposites of Ce-ZrO_2 and Al_2O_3," *J. Am. Ceram. Soc.*, **74** [12] 2979–87 (1991).

[13]D. B. Marshall, "Design of High-Toughness Laminar Zirconia Composites," *Am. Ceram. Soc. Bull.*, **71** [6] 969–73 (1992).

[14]P. E. D. Morgan and D. B. Marshall, "Ceramic Composites of Monazite and Alumina," *J. Am. Ceram. Soc.*, **78** [6] 1553–63 (1995).

[15]L. An, H. M. Chan, N. P. Padture, and B. R. Lawn, "Damage-Resistant Alumina-Based Layer Composites," *J. Mater. Res.*, **11** [1] 204–10 (1996).

[16]H. Cai, M. A. Stevens Kalceff, and B. R. Lawn, "Deformation and Fracture of Mica-Containing Glass-Ceramics in Hertzian Contacts," *J. Mater. Res.*, **9** [3] 762–70 (1994).

[17]B. R. Lawn, N. P. Padture, H. Cai, and F. Guiberteau, "Making Ceramics 'Ductile'," *Science*, **263**, 1114–16 (1994).

[18]C. K. Chyung, G. H. Beall, and D. G. Grossman, "Microstructures and Mechanical Properties of Mica Glass-Ceramics"; pp. 1167–94 in *Electron Microscopy and Structure of Materials*. Edited by G. Thomas, R. M. Fulrath, and R. M. Fisher. University of California Press, Berkeley, CA, 1972.

[19]K. Chyung, G. H. Beall, and D. G. Grossman, "Fluorophlogopite Mica Glass-Ceramics"; pp. 33–40 in *Proceedings of 10th International Glass Congress*, No. 14. Edited by M. Kunugi, M. Tashiro, and N. Saga. Ceramic Society of Japan, Kyoto, Tokyo, Japan, 1974.

[20]K. Chyung, "Fracture Energy and Thermal Shock Resistance of Mica Glass-Ceramics"; pp. 495–508 in *Fracture Mechanics of Ceramics*, Vol. 2. Edited by R. C. Bradt, D. P. H. Hasselman, and F. F. Lange. Plenum Press, New York, 1974.

[21]P. L. Swanson, "Crack-Interface Traction: A Fracture-Resistance Mechanism in Brittle Polycrystals"; pp. 135–55 in Advances in Ceramics, Vol. 22, *Fractography of Glasses and Ceramics*. Edited by J. Varner and V. D. Frechette. American Ceramic Society, Columbus, OH, 1988.

[22]C. J. Fairbanks, B. R. Lawn, R. F. Cook, and Y.-W. Mai, "Microstructure and the Strength of Ceramics"; pp. 23-37 in *Fracture Mechanics of Ceramics*, Vol. 8. Edited by R. C. Bradt, A. G. Evans, D. P. H. Hasselman, and F. F. Lange. Plenum, New York, 1986.

[23]F. Guiberteau, N. P. Padture, and B. R. Lawn, "Effect of Grain Size on Hertzian Contact in Alumina," *J. Am. Ceram. Soc.*, **77** [7] 1825–31 (1994).

[24]D. B. Marshall and B. R. Lawn, "Residual Stress Effects in Sharp-Contact Cracking: I. Indentation Fracture Mechanics, *J. Mater. Sci.*, **14** [8] 2001–12 (1979).

[25]B. R. Lawn, K. Jakus, and A. C. Gonzalez, "Sharp vs Blunt Crack Hypotheses in the Strength of Glass: A Critical Study Using Indentation Flaws," *J. Am. Ceram. Soc.*, **68** [1] 25–34 (1985).

[26]B. R. Lawn, A. G. Evans, and D. B. Marshall, "Elastic/Plastic Indentation Damage in Ceramics: The Median/Radial Crack System," *J. Am. Ceram. Soc.*, **63** [9–10] 574–81 (1980).

[27]T. P. Dabbs, B. R. Lawn, and P. L. Kelly, "A Dynamic Fatigue Study of Soda–Lime and Borosilicate Glasses Using Small-Scale Indentation Flaws," *Phys. Chem. Glasses*, **23** [2] 58–66 (1982).

[28]S. M. Wiederhorn, "Fracture Surface Energy of Glass," *J. Am. Ceram. Soc.*, **52** [2] 99–105 (1969).

[29]F. C. Frank and B. R. Lawn, "On the Theory of Hertzian Fracture," *Proc. R. Soc. London*, **A299** [1458] 291–306 (1967).

[30]B. R. Lawn and T. R. Wilshaw, "Indentation Fracture: Principles and Applications," *J. Mater. Sci.*, **10** [6] 1049–81 (1975).

[31]P. J. Kennedy, A. A. Conte, E. P. Whitenton, L. K. Ives, and M. B. Peterson, "Surface Damage and Mechanics of Fretting Wear in Ceramics"; pp. 79–98 in *Friction and Wear of Ceramics*. Edited by S. Jahanmir. Marcel Dekker, New York, 1994.

[32]H. Cai, M. A. S. Kalceff, B. M. Hooks, B. R. Lawn, and K. Chyung, "Cyclic Fatigue of a Mica-Containing Glass-Ceramic at Hertzian Contacts," *J. Mater. Res.*, **9** [10] 2654–61 (1994).

[33]K. Komvopolous, "Elastic–Plastic Finite Element Analysis of Indented Layered Media," *ASME J. Tribol.*, **111**, 430–39 (1989).

[34]F. Guiberteau, N. P. Padture, H. Cai, and B. R. Lawn, "Indentation Fatigue: A Simple Cyclic Hertzian Test for Measuring Damage Accumulation in Polycrystalline Ceramics," *Philos. Mag. A*, **68** [5] 1003–16 (1993).

[35]N. P. Padture and B. R. Lawn, "Toughness Properties of a Silicon Carbide with an *In-Situ*-Induced Heterogeneous Grain Structure," *J. Am. Ceram. Soc.*, **77** [10] 2518–22 (1994).

[36]L. M. Braun, S. J. Bennison, and B. R. Lawn, "Objective Evaluation of Short-Crack Toughness-Curves Using Indentation Flaws: Case Study on Alumina-Based Ceramics," *J. Am. Ceram. Soc.*, **75** [11] 3049–57 (1992).

[37]Y.-W. Mai and B. R. Lawn, "Crack Stability and Toughness Characteristics in Brittle Materials," *Ann. Rev. Mater. Sci.*, **16**, 415–39 (1986).

[38]D. B. Marshall, B. R. Lawn, and P. Chantikul, "Residual Stress Effects in Sharp-Contact Cracking: II. Strength Degradation," *J. Mater. Sci.*, **14** [9] 2225–35 (1979).

[39]B. R. Lawn, *Fracture of Brittle Solids*. Cambridge University Press, Cambridge, U.K., 1993.

[40]F. C. Roesler, "Brittle Fractures Near Equilibrium," *Proc. Phys. Soc. London*, **B69**, 981 (1956). □